

LINAC EFFICIENCY and BEAM QUALITIES in p, d, ${}^3_2\text{He}$ and ${}^4_2\text{He}$ ACCELERATION

JP. Auclair, PA. Chamouard, JL. Lemaire,
Laboratoire National Saturne
C.E.N. Saclay, France

Summary

Results of deuteron (d) and two helium isotopes (${}^3_2\text{He}^{2+}$ and ${}^4_2\text{He}^{2+}$) acceleration with the 20 MeV SATURNE proton linac injector, operated in the $2\beta\lambda$ mode are presented. Included are discussions of operation of the ion source, low energy beam transport transparency, longitudinal and transverse matching to the linac, linac efficiency, consequences for the high energy beam transport tuning and the best achievements.

Introduction

The 20-MeV Alvarez linear accelerator was designed to accelerate protons.¹ Over the years experimenters expressed interest for heavy ions such as deuterons and helium. Acceleration of these ions has been achieved with the present linac. As known, acceleration is possible for ions having a charge-to-mass ratio $\epsilon = z/A = \frac{1}{2}$ provided they enter the linac at the right velocity and keep in synchronism with the accelerating phase. As a consequence, the linac has to be run in the $2\beta\lambda$ -mode.^{2,3} The final kinetic energy is 5 MeV/A which is 10 MeV for deuterons, 15 MeV for ${}^3_2\text{He}$, 20 MeV for ${}^4_2\text{He}$. Good optical qualities of the accelerated ion beams were the main goal so the output current was intentionally reduced but the best performances stand respectively at 63%, 32% and 20% efficiencies for p, d, and ${}^3,4_2\text{He}$.

Injector System of Saturne 2

The injector layout is shown in Fig. 1. It shall be briefly described below.

The ion source is a duoplasmatron type housed with the accelerating column inside a pressurized preaccelerator. It delivers single charge state ions accelerated up to 800 kV, during a beam pulse of 400- μs duration, at a repetition rate of 1 Hz, for normal operation.

Since the low energy beam transport has been redesigned for a better transverse matching to the linac,⁴ higher beam brightness has been achieved. A single buncher at the fundamental frequency is installed for matching in the longitudinal phase space.

The design synchronous phase of the 200-MHz linear accelerator is 45° for the initial gaps, tapered to 25° for the final gaps. At the very end of the linac the mean energy of the beam is made to vary by 3% through the use of a 200-MHz ramping cavity to deal with the injection method.

The high energy beam transport is an entirely new design⁶ which is a strong focusing system made of triplet quadrupoles and separated achromatic sections allowing easier setup of the line. In addition to the usual beam diagnostic system a debuncher was installed which is not only sufficient for reducing energy spread but for stabilizing of the mean energy during the pulse.

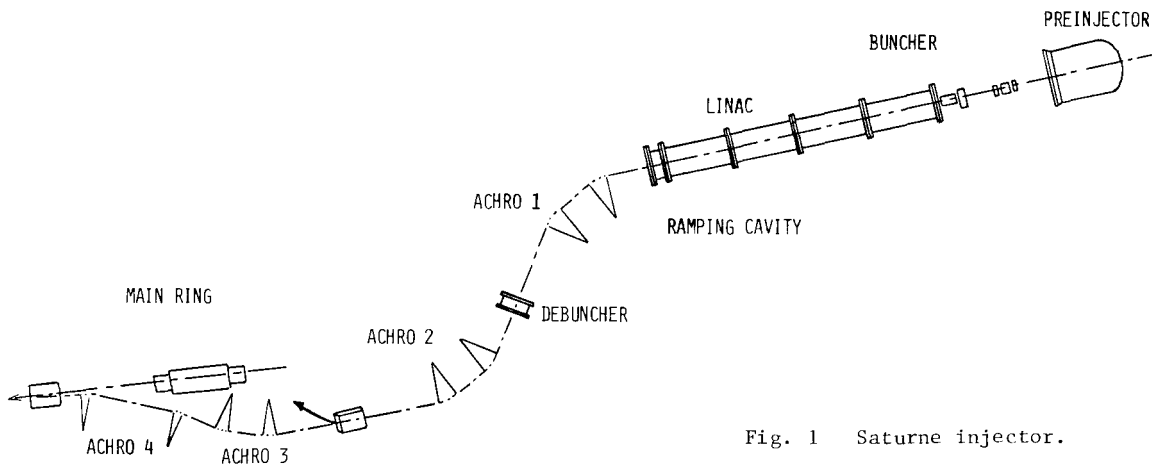


Fig. 1 Saturne injector.

Preinjector
and Low Energy Beam Transport Operation

Ion Production - Intensity Limitation

The operating mode of the preaccelerator produces single charge state ions (the duoplasmatron source gives H^+ , D^+ , ${}^3_2He^+$ and ${}^4_2He^+$); therefore one has to use a stripper for He operation. It is made of carbon foils of $10-\mu g/cm^2$ thickness, mounted on a rotating frame. A set of 14 foils will allow approximately 240 hours of running. Switching between different species takes a few hours depending upon the type of ion (residual radiation, different focusing and accelerating voltages). The measured stripper efficiency for both helium isotopes is 50%.

Let W_i be the kinetic energy of an ion beam entering the linac

$$W_i = \frac{1}{2} m_o A \beta_i^2 c^2$$

β_i is the same for all heavy ions. As mentioned above,

$$\beta_i = \frac{\beta p}{h} \quad \text{where}$$

h is the number of rf periods needed when an ion travels from one gap of the linac to the next one ($h = 2$ in the $2B\lambda$ mode). Therefore accelerating voltages and electrostatic lenses scale as $1/h^2$ while magnetic fields scale as $1/h$. Space charge however scales as $1/h^3$. The preinjector and the LEBT line have been designed to deliver 100 mA of protons at 750 kV

Table 1 gives the expected values which correspond to the scaling and the operational results for protons and deuterons.

	Protons		Deuterons	
	Design	Obs.	Calc.	Obs.
Preaccelerator Voltage (kV)	1000	750	375	375
Output Current VBI (mA)	100	40	25	25

Table 1

The corresponding results for d , 3_2He and 4_2He are given in table 2. The accelerating voltages as far as helium isotopes are concerned are higher than the scaled values due to the energy loss through the stripper carbon foil. It is in good agreement with $\frac{dE}{dx} = 2.10^3 \text{ MeV/g/cm}^2$ which is about the same for the two species.

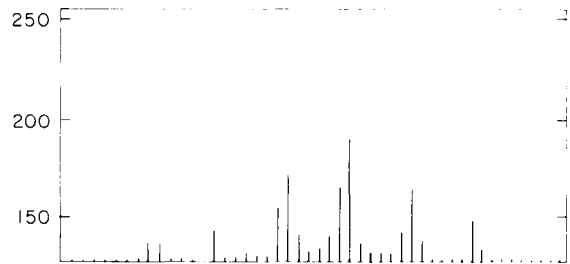
	Deuterons		${}^3_2He^+$		${}^4_2He^+$	
	Cal.	Obs.	Scaling	Oper.	Scaling	Oper.
Preaccel. Volt. (kV)	375	375	562.5	600	750	790
Output Cur. VBI (mA)	25	25	37.5	17	50	18

Table 2

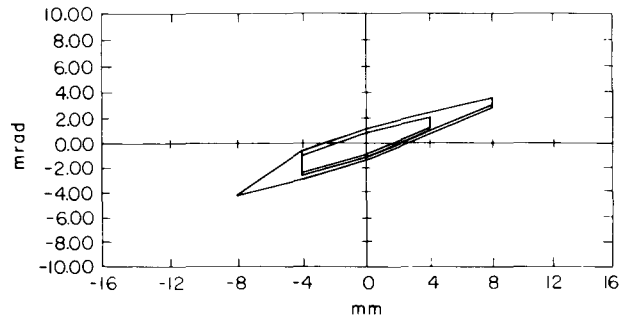
Emittance Measurement

The beam intensity is measured with either Faraday Cup current monitors (graphite plate biased by a resistor) or current transformers. Also used are aluminum oxide flags coated with CrO_2 to observe both size and shape of the beam, the beam image being displayed on a TV monitor.

The emittance is measured in the following way : the beam is masked by a graphite plate in which cylindrical holes are horizontally spaced, defining elementary beam pencils. The analysis of angles is made by a collector containing 48 copper strips deposited on an aluminium-oxide plate. This measurement is performed 6 times in the same pulse using an analog device⁷ and the results are displayed with the aid of a micro-processor. Figure 2 shows a typical display (collector spectrum and emittance contour for different thresholds).



a) collector display



b) emittance contour for different thresholds

Fig. 2 750 keV emittance measurement

The precision of the measurements is about 20% which is rather bad for an absolute value of the emittance but good enough to control the quality of the beam coming out of the ion source and emittance growth through the linac. However it has a great advantage of being very fast and giving the shape of the emittance 6 times in any single pulse, which permits quicker investigation of ion source behavior. Experimental results are given in Table 3 for different ions.

	protons	deuterons	${}^3_2\text{He}^+$	${}^4_2\text{He}^+$
beam intensity (mA)	40	25	15	16
normalized emittance for 90% & 80% of the peak distribution (mm.mrad)	2.0 1.6	0.8 0.5	0.8 0.5	1.5 1.0

Table 3

Linac Operation

Theoretical Aspect

The fundamental relationship is the energy gain per cell. The following approximation was used:

$$\Delta W_h = z e \bar{E}_h L T_h \cos \phi_h$$

where \bar{E}_h is the mean accelerating field, L the cell length and T_h the transit-time factor corresponding to the harmonic number h.

Along the accelerator $\Delta W_h = \frac{A}{h^2} \Delta W_p$, ΔW_p being the energy gain by a proton in the normal operation mode. According to this, the final energy will be

$$W_h = \frac{A}{h^2} W_p$$

Once the energy gain is fixed, it turns out that the following equation has to be satisfied in order to get acceleration.

$$E_h = \frac{1}{\epsilon h^2} \frac{\bar{E}_p T_p \cos \phi_p}{T_h \cos \phi_h}$$

with $T_h = 1/I_o \left(\frac{h\omega a}{v} \right) \sin \left(\frac{h\pi g}{L} \right) / \left(\frac{h\pi g}{L} \right)$

Actually the calculations used the correct relation for the transit-time factor because it is a crucial parameter and errors can rapidly grow too large.

$$T_h = \frac{\int_{\text{cell}} E_z \cos(2h\pi/L) dz}{\int_{\text{cell}} E_z dz}$$

The most severe limitation appears to take place in the first cells where the transit-time factor is as low as 3 times that for $\beta\lambda$ operation. This leads to very high gap voltage requirements which are beyond the possibilities of the linac and sparking is most likely to occur.

Before giving the experimental results, it is worthwhile to establish the equation for the longitudinal acceptance. For the phase it is of the order of $\Delta\phi_h \sim 3\phi_h$, taking into account the former considerations about transit time factor and maximum acceptable rf field. Then the energy acceptance becomes :

$$\Delta W_h/A = \pm 2 \sqrt{\frac{\epsilon}{h} \frac{m_o v}{\omega} e \bar{E}_h T_h f(\phi_h)}$$

where $f(\phi_h) = \phi_h \cos \phi_h - \sin \phi_h$

Experimental Results

The linac acceptance in energy and phase was measured first for protons using the usual flattened field in the $\beta\lambda$ -mode in order to have a reference, then for deuterons and ${}^3_2\text{He}^{2+}$ using the maximum power available and the calculated tilted field (Fig. 3).

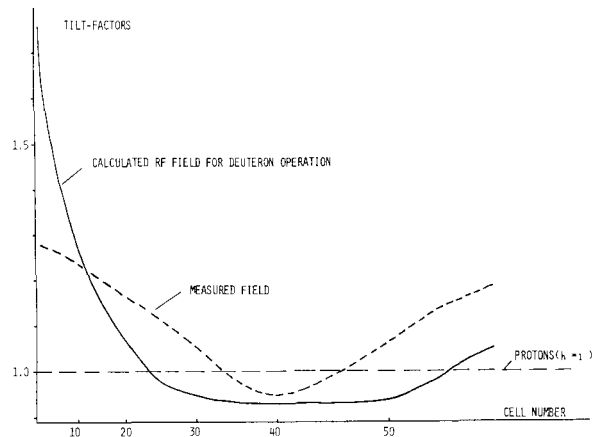


Fig. 3 Tilted rf field in $2\beta\lambda$ -mode

The experiment consisted of measuring the ratio of injected and accelerated ion current of a non-bunched beam as a function of injection energy, using downstream and upstream current transformers. Different tilted fields were tried, to deal with the previous remarks and to keep the transverse stability of the beam. Consequently, the focusing quadrupole laws had to be modified, and we had to find out a compromise between the required tilt and the maximum power available for the quadrupoles. Table 4 gives the compared results.

	p	d	${}^3_2\text{He}^{++}$	${}^4_2\text{He}^{++}$
Input C.T. (mA)	25	15	13	17
ΔW_h (keV) measured	± 90	± 25	± 50	± 80
$\Delta\phi_h$ ($^\circ$) ^c measured	100	38	39	42
$\Delta W = \frac{K}{\Delta\phi_h}$ computed	± 80	± 7	± 11	± 15
Output C.T. (mA)	13.5	4.5	2.5	3.5
Linac efficiency	52%	30%	19%	21%
Energy spread (keV)	± 125	± 85	± 110	± 140
	$\pm 62^{**}$	$\pm 30^{**}$	†	†

Table 4

** Measured with a pepper-pot of 10% transparency. Therefore the increasing is due to longitudinal space charge effects.

† Beam current leaving the pepper-pot was too small to measure.

Proton results are in good agreement with the expected values in normal operation but as far as heavy ions are concerned it is clear that the rather small phase acceptance ($\phi_h \sim 13^\circ$) does not fit with the energy acceptance results. The first conclusion is in agreement with Ref. 2 but we did not observe what they pointed out about the choice of the preaccelerator voltage.^{***} Looking at Fig. 4 where we have drawn the stable boundary defined by the rf field and dotted line representing a possible rf field taking into account an error margin, one sees that instabilities are likely to happen for cell 1 and further downstream for cells 37 to 45. Therefore losses should occur, but unfortunately we did not pursue the theoretical computation.

*** In our case, changing the preaccelerator voltage did not increase linac efficiency for deuterons like they suggested.

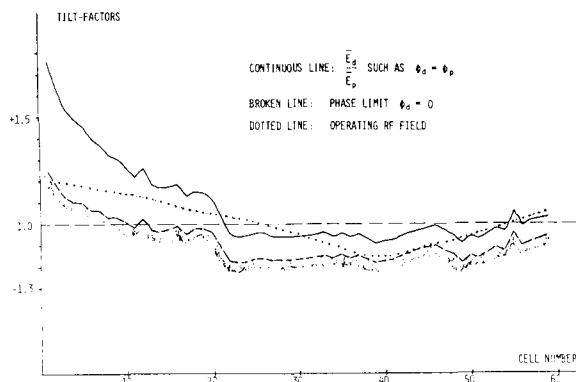


Fig. 4 Operating tilted rf field

High Energy Beam Transport Operation

Beam Optics - Beam Diagnostics

The transport line is made of 4 separated achromatic sections which can be theoretically set up independently. The elementary cell is composed of 2 bending magnets and a focusing quadrupole, the latter being movable to cope with space charge mismatching. Transverse focusing is achieved with triplet quadrupoles which bind the achromatic sections together. The last achromatic section includes an electrostatic deflector ($E = 50$ kV/cm) whose septum is a stainless steel foil of 0.5 mm thickness) and an additional quadrupole to perform both matching to the main ring and final achromatism. This strong focusing system is then easy to tune step-by-step and allows one to save time. Steering magnets are provided to properly center the beam through the line.⁸ All magnetic elements are computer controlled and computer aided operation is essential for different particles.

The beam diagnostic elements are located all along the line. It was decided to measure beam current and position in two different ways in order to improve reliability and confidence. They are very similar to the ones described previously for the LEBT.

A 39° bending magnet, inserted between achromatic section 2 and 3, allows momentum spread measurements with and without debuncher. This measurement has the disadvantage of being destructive. A graphite slit samples a beam of 0.5 mm width; the resolution of the detector is 25 keV for protons.

Emittance measurements are performed at the end of the linac using a method similar to that in LEBT. The acquisition electronics are identical for all detector devices, and allow 6 measurements in the pulse duration. Both momentum spread and emittance measurements are analyzed and displayed by the central MITRA-125 computer.⁹

Momentum Spread and Emittance Experimental Results

Momentum spread is measured after a drift length of about 10 m allowing longitudinal space charge effects to occur if they are present. Usually results are taken at 80% of the peak value (Fig. 5) and are given in Table 4. There is a constant $\Delta W/A \approx 38$ keV for deuterons and helium in rather good agreement with theory which shows that linac behavior is the same for these particles.

In addition, it is clear from the measurements with the pepper-pot, that longitudinal space charge affects momentum spread even for deuterons. Unfortunately for He^{2+} ions, the net current leaving the diluter was too small. The approximate factor of 2 measurement of momentum spread increase is also in agreement with theory and can be reduced to a more acceptable value by running the debuncher (± 150 keV for protons and less than ± 12 keV, which is the present resolution of the collector, for deuterons). The improvements of injected intensity and injection stability were straightforward.

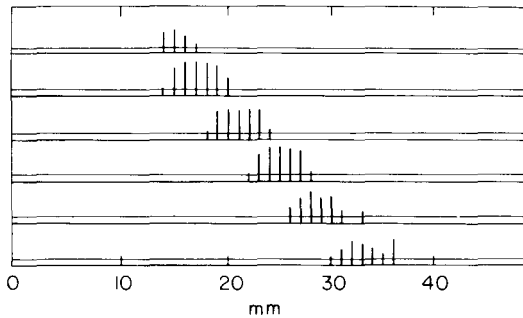


Fig. 5 Momentum spread and ramped energy display

Table 3 gave low-energy beam emittance for ${}^3_2He^+$ and ${}^4_2He^+$. Correction for multiple scattering leads to larger values for the emittance. It was evaluated using the following formula for ${}^3_2He^+$ or ${}^4_2He^+$.

$$\theta_{rms} = z \frac{15 \text{ MeV}}{p \cdot v} \frac{L}{L_{rad}}$$

where p is the mean momentum
 L is the foil thickness
 $L_{rad} = 50 \text{ g/cm}^2$ radiation length for carbon

The corresponding results are given in Table 5 where low and high energy beam emittances are compared, while emittance values versus accelerated current are plotted in Fig. 6. The transverse emittance growth is then seen to be about a factor of 2 for protons, which is a normal result according to theory, and 3 for deuterons. For He, net emittance growth is not observed, which is

certainly due to a smaller beam intensity.

		p	d	${}^3_2He^{2+}$	${}^4_2He^{2+}$
ϵ_n (LEBT)	90%	2	0.8	2.6	2.9
	(mm-mrad)	80%	1.6	0.5	2.3
ϵ_n (HEBT)	90%	5	2.7	5	-
	(mm-mrad)	80%	2.5	1.5	2.3

Table 5

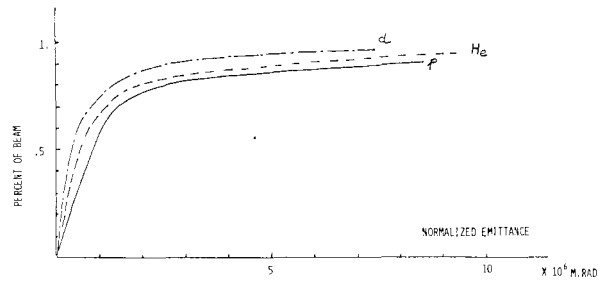


Fig. 6 Emittance versus accelerated current

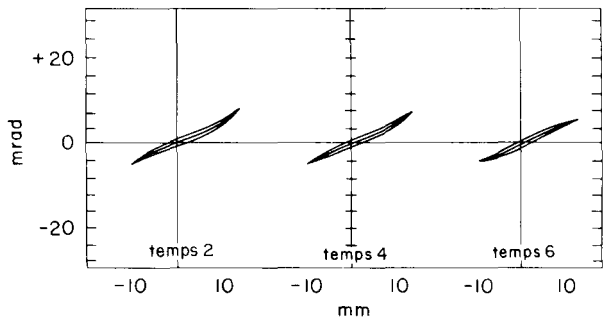


Fig. 7 HEBT emittance measurements at 3 different times in the same pulse

Conclusion

The final goal is to inject the maximum intensity of good quality beam into the main ring. Optimized proton beam led to 9.3×10^{12} injected particles using the debuncher. Also obtained was 2×10^{12} deuterons, and 1.3×10^{12} ${}^3_2He^{2+}$, without the debuncher, which was not yet running. We expect 1.6×10^{12} of ${}^4_2He^{2+}$. Making use of the debuncher, which has been recently put into operation, we should obtain a gain of 25% for these 3 species, merely by extrapolating the proton results.

References

1. JL. Lefebvre, M. Promé, "Operation report of the Saturne linac." Prof. 1970 Linac Accelerator Conference, NAL LCO-015, p.29.
2. S. Ohnuma, Th. Sluyters, "Limitations of acceleration of deuterons in Alvarez-type proton linacs." Proc. 1968 Linac Accelerator Conference, BNL 50120, p.191.
3. PA. Chamouard, JM. Lefebvre, M. Olivier, M. Prome, "Deuterons acceleration with the Saturne linac." Proc. 1972 Linac Accelerator Conference, LA-5115, p.326.
4. PA. Chamouard, M. Olivier, "Improvement in the 20-MeV beam brightness at Saturne." Proc. 1976 Linac Accelerator Conference, AECL-5677, p.372.
5. JP. Auclair, PA. Chamouard, JL. Lemaire, "200-MHz fast phase shifters and phase detection for a ramping energy." Proc. of this Conference.
6. H. Brown, J. Faure, JL. Lemaire, M. Olivier, "L'optique d'injection de Saturne II." Saclay Internal Report DSS.GERS 74-77/IE02 17/01/1974.
7. JM. Lagniel, "Rapport de stage." Saclay Internal Report DDS.985 15/06/1976.
8. D. Moro, M. Olivier, "Etude de la ligne de transport de Saturne II." Saclay Internal Report DSS.GERMA 75-50/IE 83 04/08/1975.
9. F. Mathy, "Traitement informatique des mesures par capteur à fil sur la ligne d'injection." Saclay Internal Report LNS/SD AS 11/10 DMA 05 06/08/1979.

DISCUSSION

R.W. Hamm, LASL: What are the electron beam current and energy for the results that you have given? Are these the same current and voltage for the results at the 1979 Particle Accelerator Conference?

Lemaire: Yes, 250 mA, 4 kV.

D. Bohne, GSI: The intensity figures you gave us, are they relevant for the output of the synchrotron or during the injection pulse?

Lemaire: They apply to the injection pulse.

E. Parker, ANL: What was the deuteron polarization?

Lemaire: The results have been obtained just a few days ago and I do not have the value yet.